Structural Characterization of Triacylglycerols as Lithiated Adducts by Electrospray Ionization Mass Spectrometry Using Low-Energy Collisionally Activated Dissociation on a Triple Stage Quadrupole Instrument

Fong-Fu Hsu and John Turk

Mass Spectrometry Resource, Division of Diabetes, Endocrinology and Metabolism, Department of Medicine, Washington University School of Medicine, St. Louis, Missouri, USA

We describe features of tandem mass spectra of lithiated adducts of triacylglycerol (TAG) species obtained by electrospray ionization mass spectrometry (ms) with low-energy collisionally activated dissociation (CAD) on a triple stage quadrupole instrument. The spectra distinguish isomeric triacylglycerol species and permit assignment of the mass of each fatty acid substituent and positions on the glycerol backbone to which substituents are esterified. Source CAD-MS^2 experiments permit assignment of double bond locations in polyunsaturated fatty acid substituents. The ESI/MS/MS spectra contain $[M + Li - (R_nCO_2H)]^+$, $[M + Li - (R_nCO_2Li)]^+$, and R_nCO^+ ions, among others, that permit assignment of the masses of fatty acid substituents. Relative abundances of these ions reflect positions on the glycerol backbone to which substituents are esterified. The tandem spectra also contain ions reflecting combined elimination of two adjacent fatty acid residues, one of which is eliminated as a free fatty acid and the other as an α,β-unsaturated fatty acid. Such combined losses always involve the sn-2 substituent, and this feature provides a robust means to identify that substituent. Fragment ions reflecting combined losses of both sn-1 and sn-3 substituents without loss of the sn-2 substituent are not observed. Schemes are proposed to rationalize formation of major fragment ions in tandem mass spectra of lithiated TAG that are supported by studies with deuterium-labeled TAG and by source CAD-MS^2 experiments. These schemes involve initial elimination of a free fatty acid in concert with a hydrogen atom abstracted from the α-methylene group of an adjacent fatty acid, followed by formation of a cyclic intermediate that decomposes to yield other characteristic fragment ions. Determination of double bond location in polyunsaturated fatty acid substituents of TAG is achieved by source CAD experiments in which dilithiated adducts of fatty acid substituents are produced in the ion source and subjected to CAD in the collision cell. Product ions are analyzed in the final quadrupole to yield information on double bond location. (J Am Soc Mass Spectrom 1999, 10, 587–599) © 1999 American Society for Mass Spectrometry

Triacylglycerols (TAG) are important long-term fuel storage molecules, and each molecule contains three fatty acid substituents esterified to a glycerol backbone. An individual TAG molecule may contain up to three distinct fatty acid substituents, each of which can have varying chain lengths, degrees of unsaturation, and locations of double bonds. Although TAG have long been viewed as passive storage molecules, recent evidence suggests that they must be present at some minimal levels within certain cells, such as pancreatic islet beta cells, to support specialized functions and that accumulation of high levels of TAG impairs such functions [1–3]. It is not known whether such effects depend only on TAG amount or are also influenced by TAG molecular composition. Under some conditions, accumulation of unusual TAG species, such as triarachidonin, can be induced [4].

Whether accumulation of unusual TAG species adversely affects beta cell function is an important question because insulin secretion by beta cells is impaired in type II diabetes mellitus, and disturbances of fatty acid and TAG metabolism precede the insulin secretory defect in human and rodent type II diabetes [1–3, 5, 6]. Rodent islets also accumulate abnormally large amounts of TAG as the insulin secretory defect evolves [1–3]. Existing information on islet TAG derives from methods involving hydrolysis to glycerol and free fatty acids [1–3], which cannot determine the structures of

Address reprint requests to John Turk, Box 8127, Washington University School of Medicine, 660 S. Euclid Ave., St. Louis, MO 63110. E-mail: jturk@imgate.wustl.edu

1044-0305/99/$20.00
PII S1044-0305(99)00035-5

Received November 2, 1998
Revised January 14, 1999
Accepted March 23, 1999

intact TAG molecules. Because islets are obtainable in only small quantities, structural determination of islet complex lipids is difficult, and highly sensitive electrospray ionization (ESI) mass spectrometric (MS) methods have proven valuable in characterizing islet glycerophospholipids and sphingolipids [7, 8]. We have therefore examined whether ESI/MS/MS is similarly useful in determining TAG structures to develop methods applicable to the small quantities of TAG in islets.

Our studies have been influenced by previous mass spectrometric approaches to TAG characterization involving various ionization methods, including electron impact [9–11], chemical ionization [9, 12–23], field desorption [24, 25], desorption chemical ionization [26–28], fast atom bombardment (FAB) [29–31], thermospray [32, 33], electrospray ionization (ESI) [34–37], and atmospheric pressure chemical ionization [38–44]. Such techniques can determine TAG molecular weights and, when combined with collisionally activated dissociation (CAD) and tandem mass spectrometry, can identify the mass of each fatty acid substituent, from which their chain lengths and degrees of unsaturation can be inferred. It is more difficult to determine the positions of fatty acid substituents on the glycerol backbone and the locations of double bonds within fatty acid chains.

Complete structural characterization of TAG as sodiated adducts by FAB/MS/MS using high-energy CAD on a multisector mass spectrometer has recently been achieved [35]. The tandem mass spectra generated from CAD of $[M + Na]^+$ ions produced by FAB yielded sufficient information to determine the mass of each fatty acid substituent, positions of fatty acid substituents on the glycerol backbone, and double bond locations in unsaturated substituents [35]. ESI/MS/MS analyses of cationized TAG under conditions of high-energy CAD on a multisector instrument indicated that sodiated adducts were unsatisfactory because of rapid diminution in $[M + Na]^+$ ion abundance, but $[M + NH_4]^+$ ions of ammoniated adducts yielded a stable ion current during continued infusion [35]. High-energy CAD of TAG $[M + NH_4]^+$ ions yielded ESI/MS/MS spectra that identified the fatty acid substituents, including the locations of double bonds in unsaturated substituents, but these spectra did not identify the position of the fatty acid substituents on the glycerol backbone [35]. The combination of ESI/MS/MS of TAG $[M + NH_4]^+$ ions and FAB/MS/MS of $[M + Na]^+$ ions using high-energy CAD was found be useful in TAG characterization, with the former offering both better sensitivity and the potential for combination with liquid chromatography (LC) separation and the latter offering more detailed structural information [35].

ESI/MS/MS using low-energy CAD on a tandem quadrupole instrument has also been used to characterize TAG in experiments involving infusion in chloroform/methanol solutions containing sodium acetate or ammonium acetate to yield $[M + Na]^+$ or $[M + NH_4]^+$ ions, respectively [34]. Low-energy CAD tandem mass spectra of TAG $[M + Na]^+$ ions did not contain abundant, structurally informative fragment ions, but CAD spectra of $[M + NH_4]^+$ ions contained abundant product ions, such as $[M - (R_nCO_2NH_4)]^+$, $[R_nCO + 74]$ and R_nCO^+, that identified the mass of each fatty acid substituent [34]. Neither the positions of the fatty acid substituents on the glycerol backbone nor the locations of double bonds in unsaturated fatty acid substituents could be determined from these spectra [34].

We have reported that formation of lithiated adducts of glycerophosphocholine (GPC) lipids facilitates assignments of the identifies and positions of their fatty acid substituents by ESI/MS/MS using low-energy CAD on a triple stage quadrupole instrument [45]. We report here that this approach is also useful in determining identities and positions of fatty acid substituents in TAG. Infusion of TAG in solutions containing lithium acetate yields abundant $[M + Li]^+$ ions on ESI/MS, and the ion current is stable over hours of infusion. Low-energy CAD tandem spectra of TAG $[M + Li]^+$ ions contain product ions that identify the mass of each fatty acid substituent, and the relative abundances of these ions identify the locations of these substituents on the glycerol backbone. Under conditions of source CAD, dilithiated adducts of fatty acid substituents are produced from TAG molecules, and CAD of these ions yields spectra that contain product ions that identify double bond locations in unsaturated substituents.

Experimental

Material and Chemicals

Synthetic triacylglycerol standards rac-glyceryl-1,3-dipalmitate-2-oleate [(16:0/18:1/16:0)-TAG], rac-glyceryl-2,3-dipalmitate-1-oleate [(18:1/16:0/16:0)-TAG], rac-glyceryl-1-palmitate-2-oleate-3-stearate [(16:0/18:1/18:0)-TAG], rac-glyceryl-1-palmitate-2-stearate-3-oleate [(16:0/18:0/18:1)-TAG], rac-glyceryl-1,3-distearate-2-oleate [(18:0/ 18:1/18:0)-TAG], rac-glyceryl-2,3-distearate-1-oleate [(18:1/18:0/18:0)-TAG], and tripalmitin [(16:0/16:0/16:0)-TAG] were purchased from Matreya (Pleasant Gap, PA). The synthetic triacylglycerol standards triarachidonin [(20:4/20:4/20:4)-TAG] and trilinolein [(18:2/18:2/18:2)-TAG] were purchased from NuChek Prep (Elysian, MN). The deuterium-labeled triacylglycerol standards tripalmitin-d_{31} [(d_{31}16:0/d_{31}16:0/d_{31}16:0)-TAG] and glyceryl tri(hexadecanoate-2,2-d_2) [($d_2$16:0/$d_2$16:0/$d_2$16:0)-TAG] were purchased from C/D/N Isotopes (Quebec, Canada). All solvents and other chemicals were obtained from Fisher Chemical.

Mass Spectrometry

ESI/MS analyses were performed on a Finnigan TSQ-7000 triple stage quadrupole mass spectrometer equipped with an electrospray ion source and controlled by Finnigan ICIS software operated on a DEC alpha station. Standard triacylglycerols were dissolved

in chloroform/methanol (1/4) at final concentration of 10 pmol/μL. Lithium acetate was then added to this solution to achieve a final [Li^+] of 2 mM. Samples were infused (1 μL/min) into the ESI source with a Harvard syringe pump. The electrospray needle and the skimmer were operated at ground potential and the electrospray chamber and the entrance of the glass capillary at 4.5 kV. The heated capillary temperature was 250 °C. Ions of interest were selected in the first quadrupole and accelerated (collision energy 40–50 eV) into a collision cell containing argon (2.3 mtorr) to induce CAD. Product ions were then analyzed in the final quadrupole. For source CAD experiments, the skimmer voltage was set at 50–60 V to induce fragmentation within the ion source. Selected fragment ions were then isolated in the first quadrupole and accelerated (collision energy 25–35 eV) into the collision cell containing argon (2.3 mtorr) to yield second generation fragment ions, which were then analyzed in the final quadrupole.

Results

Determination of the Identities of Fatty Acid Substituents in Triacylglycerol Species

When infused into the ion source in solutions containing 2 mM lithium acetate, TAG species yielded abundant $[M + Li]^+$ ions on ESI/MS, and the ion current was stable over hours of infusion. Upon CAD, $[M + Li]^+$ ions yielded abundant fragment ions that reflect the identities and positions of the fatty acid substituents. Fragment ions that reflect the mass of each fatty acid substituent are observed at *m/z* values corresponding to $[M + Li - (R_nCO_2H)]^+$ and $[M + Li - (R_nCO_2Li)]^+$, where *n* denotes the glycerol carbon to which the fatty acid is esterified. For example, the CAD tandem spectra of lithiated adducts of (16:0/18:0/18:1)-TAG (Figure 1A) and of (16:0/18:1/18:0)-TAG (Figure 1B) contain ions at *m/z* 611, 583, and 585, reflecting neutral loss of palmitic acid (16:0), stearic acid (18:0), or oleic acid (18:1), respectively, from $[M + Li]^+$. Ions at *m/z* 605, 577, and 579 reflect neutral losses of the lithium salts of these fatty acids from $[M + Li]^+$.

The mass of each fatty acid substituent is also reflected by $[R_nCO_2H + Li]^+$, R_nCO^+, and $[R_nCO^+ - 18]$ fragment ions in the tandem spectra of lithiated adducts of TAG. In Figure 1, $[R_nCO_2H + Li]^+$ ions for the fatty acid substituents 18:0, 18:1, and 16:0 occur at *m/z* 291, 289, and 263, respectively. The acylium (R_nCO^+) ions derived from 18:0, 18:1, and 16:0 occur at *m/z* 267, 265, and 239, respectively, and the corresponding $[R_nCO^+ - 18]$ ions occur at 249, 247, and 221, respectively.

Determination of the Position of Fatty Acid Substituents on the Glycerol Backbone of TAG Species

Fragment ions reflecting neutral loss of the sn-2 fatty acid substituent either as a free fatty acid or as a lithium salt were less abundant than the corresponding ions reflecting such losses of either the sn-1 or the sn-3 fatty acid substituent. In Figure 1A, for example, the ions at *m/z* 585 and 611 reflect neutral losses of the sn-1 substituent 16:0 or the sn-3 substituent 18:1, respectively, as a free fatty acid. Both of those ions are of similar abundance, and each is about 1.5-fold more abundant than the ion at *m/z* 583, which reflects neutral loss of the sn-2 substituent 18:0 as a free fatty acid. Similar relationships are observed in comparisons with the intensities of ions reflecting losses of the fatty acid substituents as lithium salts. The ion (*m/z* 577) reflecting loss of the sn-2 substituent 18:0 as a lithium salt is less intense than the ions at *m/z* 605 or 579 reflecting loss of the sn-1 substituent 16:0 or the sn-3 substituent 18:1, respectively, as lithium salts (Figure 1A).

Comparison of Figure 1B and Figure 1A, which are tandem spectra of lithiated adducts of two positionally isomeric TAG species with identical fatty acid substituents, illustrates that it is the position of the fatty acid substituent on the glycerol backbone and not the identity of the fatty acid that governs the relative abundances of ions that reflect losses of fatty acid substituents as free fatty acids or as lithium salts. In Figure 1B, the ions at *m/z* 611 and 583 reflecting loss of the sn-1 or sn-3 substituent, respectively, as free fatty acids are of similar abundance, and each is about 1.5-fold more abundant than the ion at *m/z* 585 reflecting loss of the sn-2 substituent as a free fatty acid. Similar relation-

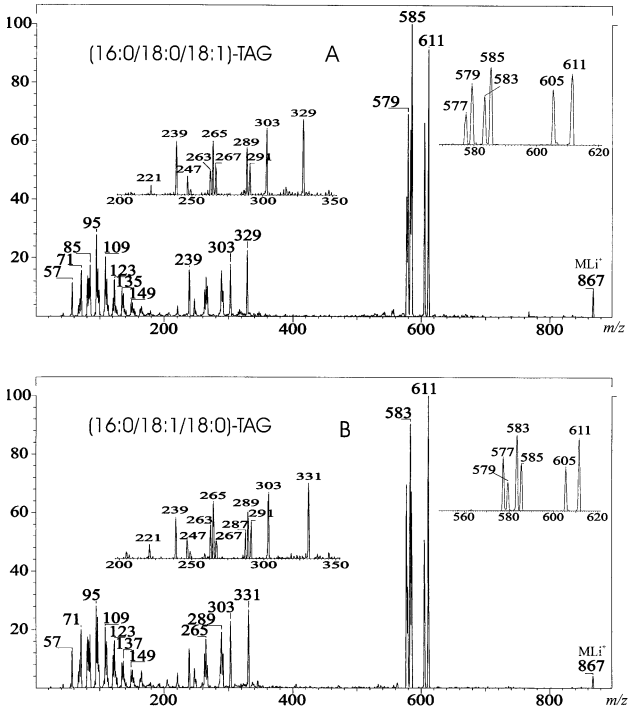

Figure 1. Tandem mass spectra of lithiated adducts of two positionally isomeric TAG species that contain three distinct fatty acid substituents. Panels **A** and **B** are tandem spectra of the lithiated adducts of (16:0/18:0/18:1)-TAG and of (16:0/18:1/18:0)-TAG, respectively.

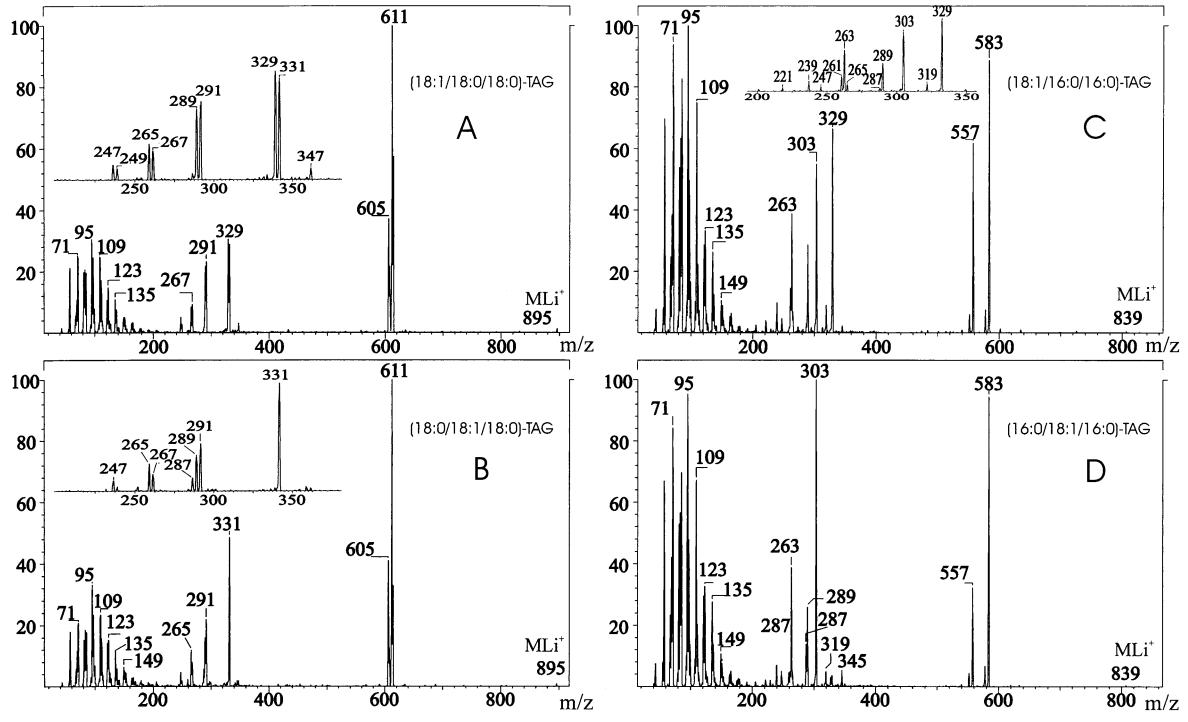

Figure 2. Tandem mass spectra of lithiated adducts of two sets of positionally isomeric TAG species with different sn-2 fatty acid substituents. Panel **A** is the tandem spectrum of the lithiated adduct of (18:1/18:0/18:0)-TAG and panel **B** that of its positional isomer (18:0/18:1/18:0)-TAG. Panel **C** is the tandem spectrum of the lithiated adduct of (18:1/16:0/16:0)-TAG and panel **D** that of its positional isomer (16:0/18:1/16:0)-TAG.

ships are observed when comparing the relative intensities of ions reflecting loss of the fatty acid substituents as lithium salts at *m/z* 605 and 577 for the sn-1 and sn-3 substituents, respectively, and at *m/z* 579 for the sn-2 substituent (Figure 1B).

Two other characteristic ions in the tandem spectra of lithiated adducts of TAG reflect the combined loss of either the sn-1 or sn-3 substituent and the loss of the sn-2 substituent. One of the substituents is eliminated as a free fatty acid and the other as an α,β-unsaturated fatty acid. (Grounds for assigning an α,β-position to the new site of unsaturation in the eliminated fatty acid substituent are considered in the Discussion section. To follow arguments developed in the Results section, it is important to recognize only that the second fatty acid eliminated has a new site of unsaturation.) The two resultant ions are of approximately equal abundance and yield a pair separated in *m/z* value by the difference in masses between the sn-1 and sn-3 substituents. In Figure 1A for (16:0/18:0/18:1)-TAG, this pair occurs at *m/z* 329 [M + Li − (R_1CO_2H) − ($R'_2CH{=}CHCO_2H$)] and *m/z* 303 [M + Li − (R_3CO_2H) − ($R'_2CH{=}CHCO_2H$)]. The difference between 329 and 303 is 26, and that is also the difference in mass between the sn-1 substituent palmitic acid (MW 256) and the sn-3 substituent oleic acid (MW 282). Similarly, in Figure 1B for the positional isomer (16:0/18:1/18:0)-TAG, the corresponding pair of ions occurs at *m/z* 331 [M + Li − (R_1CO_2H) − ($R'_2CH{=}CHCO_2H$)] and *m/z* 303 [M + Li − (R_3CO_2H) − ($R'_2CH{=}CHCO_2H$)]. The difference between 331 and 303 is 28, and that is also the difference in mass between the sn-1 substituent palmitic acid (MW 256) and the sn-3 substituent stearic acid (MW 284). Such ion pairs identify the sn-2 substituent because that substituent is lost from both members of the pair.

There are no analogous ions of high abundance in the tandem spectra of lithiated adducts of TAG species that reflect combined losses of both the sn-1 and sn-3 substituents. For example, in the tandem spectrum for (16:0/18:1/18:0)-TAG in Figure 1B, an ion reflecting loss of both the sn-1 and sn-3 substituents as free fatty acids would exhibit an *m/z* value of 327, and an ion reflecting loss of one of those substituents as a free fatty acid and the other as an α,β-unsaturated fatty acid would exhibit an *m/z* value of 329. There are no abundant ions at *m/z* 327 or 329 in the spectrum in Figure 1B. Ions that reflect loss of two fatty acid substituents from a lithiated TAG species have therefore always undergone loss of the sn-2 substituent, and the presence of a pair of such ions identifies the sn-2 substituent.

That these distinctive losses involving the sn-2 substituent can be used to distinguish positional isomers and to assign the identity of the sn-2 substituent in TAG species is further illustrated by the tandem spectra for two additional pairs of positional isomers in Figure 2. Panels A and B are the tandem spectra of the lithiated adducts of the positional isomers (18:1/18:0/18:0)-TAG and (18:0/18:1/18:0)-TAG, respectively. In the former,

the difference in mass between the sn-1 substituent (oleic acid, MW 282) and the sn-3 substituent (stearic acid, MW 284) is 2, and a pair of ions that differ in *m/z* value by 2 units is observed at *m/z* 331 and 329 (Figure 2A, see magnified inset). These ions correspond to [M + Li − (R_1CO_2H) − ($R'_2CH{=}CHCO_2H$)] and to [M + Li − (R_3CO_2H) − ($R'_2CH{=}CHCO_2H$)], respectively. In contrast, for (18:0/18:1/18:0)-TAG, the sn-1 and sn-3 substituents are identical, and there is no difference in mass between them. The tandem spectrum of this compound therefore contains a single ion (*m/z* 331) in the *m/z* region where ions reflecting loss of two fatty acid substituents are represented (Figure 2B). This ion corresponds to [M + Li − (R_nCO_2H) − ($R'_2CH{=}CHCO_2H$)], where *n* is either 1 or 3.

The tandem spectra of the lithiated adducts of the positional isomers (18:1/16:0/16:0)-TAG (Figure 2C) and (16:0/18:1/16:0)-TAG (Figure 2D) again illustrate this phenomenon. In the former, the difference in mass between the sn-1 substituent (oleic acid, MW 282) and the sn-3 substituent (palmitic acid, MW 256) is 26, and an ion pair separated by 26 *m/z* units is observed at *m/z* 303 and 329. These ions correspond to [M + Li − (R_1CO_2H) − ($R'_2CH{=}CHCO_2H$)] and [M + Li − (R_3CO_2H) − ($R'_2CH{=}CHCO_2H$)], respectively. In contrast, for (16:0/18:1/16:0)-TAG, the sn-1 and sn-3 substituents are identical, and there is no difference in mass between them. The tandem spectrum of this compound therefore contains a single ion (*m/z* 303) in the *m/z* region where ions reflecting loss of two fatty acid substituents are represented. This ion corresponds to [M + Li − (R_nCO_2H) − ($R'_2CH{=}CHCO_2H$)], where *n* is either 1 or 3.

The formation of an α,β-unsaturated fatty acid from the sn-2 substituent in lithiated TAG species under conditions of low-energy CAD is also reflected by the presence of [$R'_2CH{=}CHCO_2H$ + Li]$^+$ ions in the tandem spectra. Such an ion is present at *m/z* 287 in the spectra in Figures 1B and 2B, D and at *m/z* 261 in the spectrum in Figure 2C. In the spectra in Figures 1A and 2A, ions with the appropriate *m/z* value for [$R'_2CH{=}CHCO_2H$ + Li]$^+$ are also present at *m/z* 289, but there is also a contribution from [oleic acid + Li]$^+$ to the ion current at this *m/z* value because oleic acid is the sn-3 or the sn-1 substituent in the lithiated TAG for which tandem spectra are displayed in Figure 1A or 2A, respectively.

Scheme **1**A, which is discussed in detail in the Discussion section, proposes a route to the sequential elimination of an outer (sn-1 or sn-3) fatty acid substituent followed by elimination of the sn-2 substituent as an α,β-unsaturated fatty acid. The Scheme proposes that the members of the ion pair reflecting combined elimination of two adjacent fatty acid residues from the TAG [M + Li]$^+$ ion represent lithium adducts of allyl esters of the sn-1 substituent and of the sn-3 substituent, respectively. This indicates that the masses of the outer fatty acid substituents can be determined by subtracting 47 from the *m/z* values of the members of the ion pair

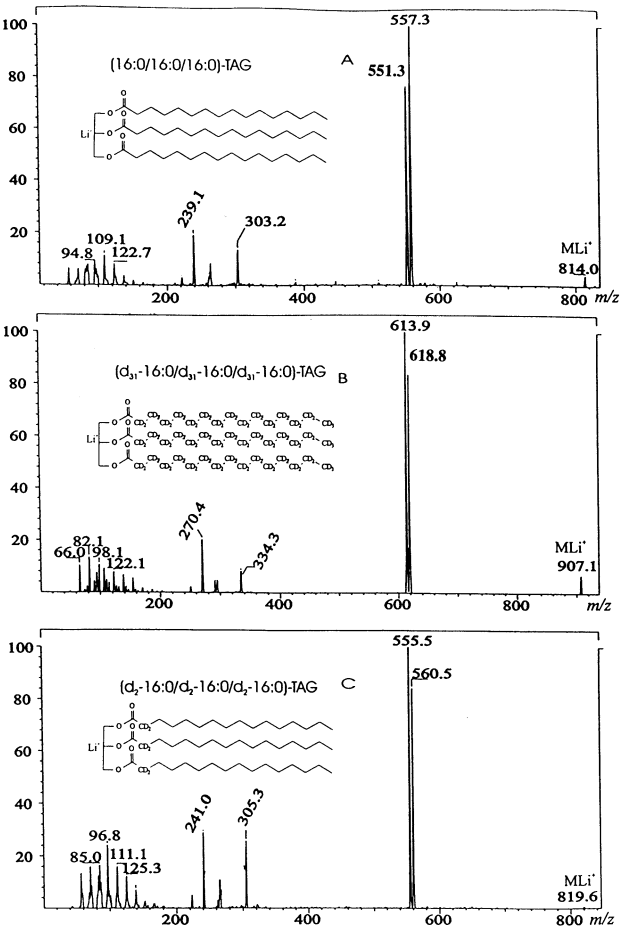

Figure 3. Tandem mass spectra of lithiated adducts of tripalmitin species that contain unlabeled palmitic acid substituents or contain palmitic acid substituents labeled with deuterium atoms in the fatty acid chain. Panel **A** is the tandem spectrum of the lithiated adduct of (16:0/16:0/16:0)-TAG, panel **B** that of (d_{31}16:0/d_{31}16:0/d_{31}16:0)-TAG, and panel **C** that of ($d_2$16:0/$d_2$16:0/$d_2$16:0)-TAG. In panels **B** and **C**, positions of deuterium atoms are specified on structural diagrams. The compound in panel **A** contains no deuterium label.

reflecting combined elimination of two adjacent fatty acid substituents. This Scheme is supported by studies with deuterium-labeled TAG species and with source CAD-MS^2 experiments that are considered in the immediately following Results sections.

Studies with TAG Species Containing Deuterium-Labeled Fatty Acids to Identify the Source of Hydrogen Atoms Eliminated with Fatty Acid Residues upon CAD of Lithiated Adducts

Figure 3A, B represent tandem spectrum of lithiated adducts of (16:0/16:0/16:0)-TAG and of (d_{31}16:0/d_{31}16:0/d_{31}16:0)-TAG, respectively. In the latter compound, all three palmitic acid substituents are perdeuterated. The calculated mass of the [M + Li]$^+$ ion of (16:0/16:0/16:0)-TAG − Li^+ is 813.7, and loss of unlabeled palmitic acid (MW 256.2) should yield a fragment

ion at 557.5, which is quite close to the observed value at 557.3 (Figure 3A). The members of the ion pair reflecting loss of a palmitic acid (*m/z* 557.3) or its lithium salt (*m/z* 551.3) from $[M + Li]^+$ are also separated in *m/z* value by the expected 6 units, reflecting the difference between the mass of a lithium ion and a proton (Figure 3A). The calculated mass of the lithiated adduct of (d_{31}16:0/d_{31}16:0/d_{31}16:0)-TAG is 907.3. Loss of perdeuterated 16:0 as a free fatty acid with a ^1H or a ^2H atom on the carboxylic acid moiety should result in a loss of 284.4 or 285.4, respectively, yielding a fragment ion at *m/z* 619.9 or 618.9, respectively. The observed *m/z* value (618.8) for this fragment ion in Figure 3B indicates that the fatty acid has been eliminated with an atom of ^2H and not ^1H. This is supported by the fact that the difference in *m/z* values between members of the ion pair reflecting elimination of the sn-2 substituent as a free fatty acid (*m/z* 618.8) or as a lithium salt (*m/z* 613.9) is about 5 units rather than the 6 units expected if the free fatty acid had been eliminated with a ^1H atom (Figure 3B).

Because there are no ^2H atoms bonded to glycerol carbon atoms in (d_{31}16:0/d_{31}16:0/d_{31}16:0)-TAG, the ^2H eliminated with the fatty acid must have been abstracted from a C–^2H bond in another fatty acid substituent in the TAG molecule. The spectrum in Figure 3C indicates that this ^2H atom is derived from an α-methylene group of a fatty acid substituent. Figure 3C is the tandem spectrum of the lithiated adduct of ($d_2$16:0/$d_2$16:0/$d_2$16:0)-TAG, in which each fatty acid substituent bears two ^2H atoms on its α-methylene group but is not labeled elsewhere. The *m/z* value for the fragment ion reflecting loss of a fatty acid substituent as a free fatty acid should occur at *m/z* 561.5 or at *m/z* 560.5 if the fatty acid is eliminated with a ^1H or ^2H atom, respectively. The observed *m/z* value (560.5) matches the latter value, indicating that the fatty acid is eliminated with a ^2H atom. This is supported by the 5 unit difference in *m/z* value between the ions reflecting elimination of the free fatty acid (*m/z* 560.5) or its lithium salt (*m/z* 555.5) from $[M + Li]^+$. This difference corresponds to that between the mass of ^2H and Li rather than to that between ^1H and Li. These observations indicate that elimination of free fatty acids from lithiated adducts of TAG species involves abstraction of a hydrogen atom from the α-methylene group of another fatty acid residue in the molecule.

Source CAD-MS^2 Experiments to Examine the Genesis of Ions Observed in the Tandem Mass Spectra of Lithiated Adducts of TAG Species

In these experiments, an offset potential of 50–60 V was applied to the skimmer to induce fragmentation of the parent ions in the ion source. Fragment ions of interest were then selected in the first quadrupole and subjected to CAD in the collision cell to yield second generation fragment ions. These ions were then analyzed in the final quadrupole to obtain MS^2 spectra.

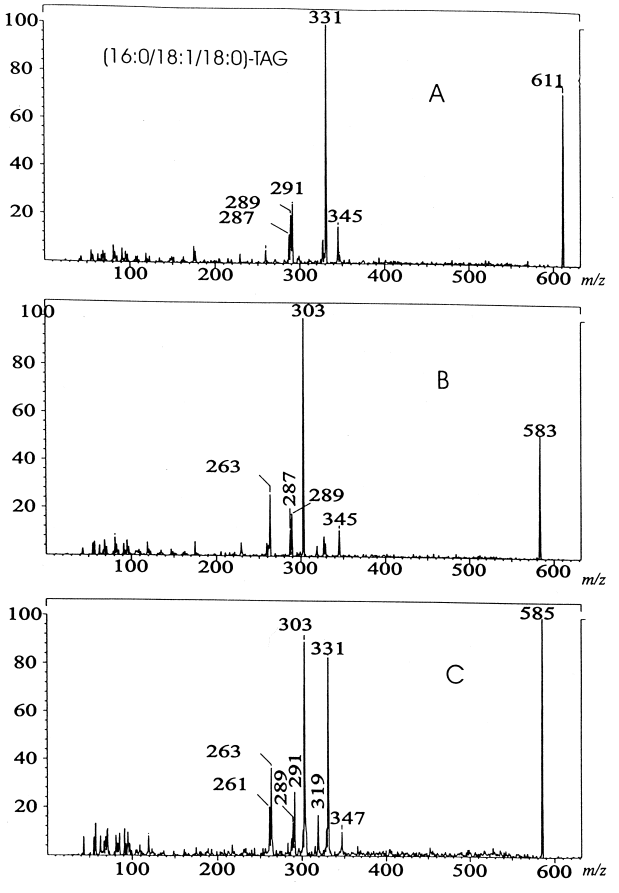

Figure 4. Source CAD-MS^2 spectra obtained from first generation fragment ions arising from loss of fatty substituents from the lithiated adduct of rac-glyceryl-1-palmitate-2-oleate-3-stearate as free fatty acids. Each spectrum was obtained under conditions of source CAD of parent (16:0/18:1/18:0)-TAG. First generation fragment ions were selected in the first quadrupole and subjected to CAD in the collision cell to yield second generation fragment ions, which were analyzed in the final quadrupole to obtain MS^2 spectra. Panels **A**, **B**, and **C** represent MS^2 spectra obtained from first generation product ions at *m/z* 611, 583, and 585, respectively. These first generation product ions arise from loss of the sn-1, sn-3, or sn-2 substituents, respectively, as free fatty acids from the parent $[M + Li]^+$ ion.

The sequence of events in the genesis of fragment ions that reflect combined losses of an outer (sn-1 or sn-3) fatty acid substituent and of the sn-2 substituent were first examined with lithiated adducts of the positional isomers (16:0/18:1/18:0)-TAG (Figure 4) and (16:0/18:0/18:1)-TAG (Figure 5). In Figure 4, fragment ions generated in the source that reflected loss from $[M + Li]^+$ of the sn-1 (panel A), sn-3 (panel B), or sn-2 (panel C) substituents as free fatty acids were isolated in the first quadrupole and subjected to CAD. Figure 4A illustrates that the most abundant product ion (*m/z* 331) from the $[M + Li - R_1CO_2H]^+$ ion represents the fragment generated by loss of the sn-2 substituent as an α,β-unsaturated fatty acid. In addition, $[R'_2CH{=}CHCO_2H + Li]^+$ (*m/z* 287), $[R_2CO_2H + Li]^+$ (*m/z* 289), and $[R_3CO_2H + Li]^+$ (*m/z* 291) ions are observed.

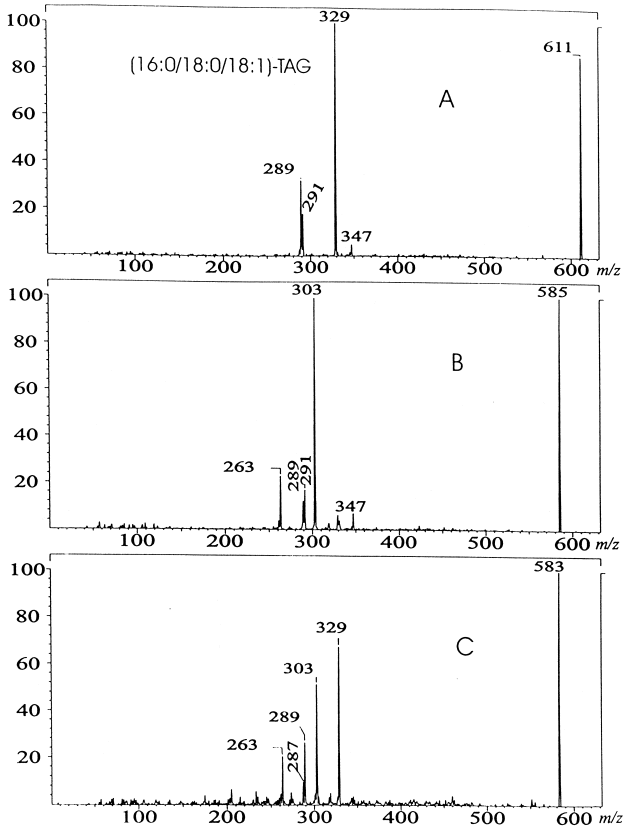

Figure 5. Source CAD-MS^2 spectra obtained from first generation fragment ions arising from loss of fatty substituents from the lithiated adduct of rac-glyceryl-1-palmitate-2-stearate-3-oleate as free fatty acids. Each spectrum was obtained under conditions of source CAD of parent (16:0/18:0/18:1)-TAG. First generation fragment ions were selected in the first quadrupole and subjected to CAD in the collision cell to yield second generation fragment ions, which were analyzed in the final quadrupole to obtain MS^2 spectra. Panels **A**, **B**, and **C** represent MS^2 spectra obtained from first generation product ions at *m/z* 611, 585, and 583, respectively. These first generation product ions arise from loss of the sn-1, sn-3, or sn-2 substituents, respectively, as free fatty acids from the parent $[M + Li]^+$ ion.

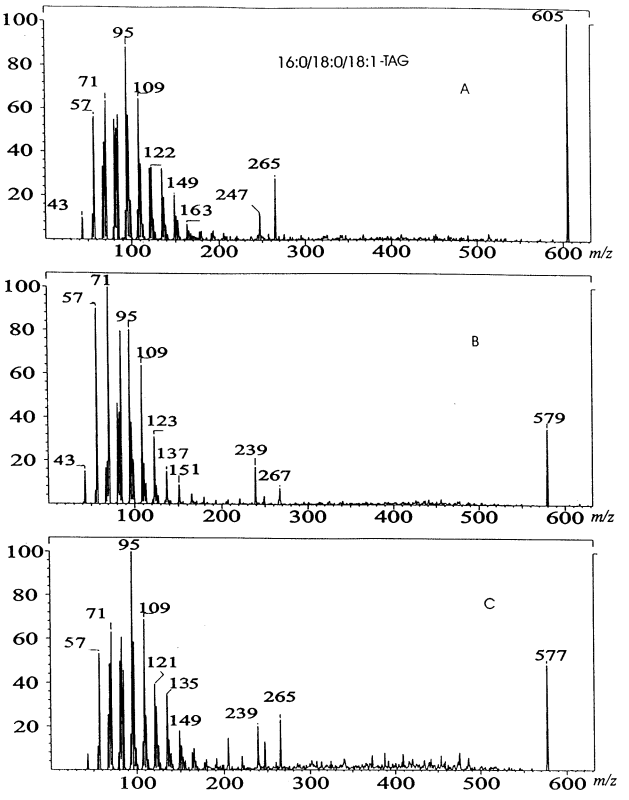

Figure 6. Source CAD-MS^2 spectra obtained from first generation fragment ions arising from loss of fatty substituents from the lithiated adduct of rac-glyceryl-1-palmitate-2-stearate-3-oleate as lithium salts. Each spectrum was obtained under conditions of source CAD of parent (16:0/18:0/18:1)-TAG. First generation fragment ions were selected in the first quadrupole and subjected to CAD in the collision cell to yield second generation fragment ions, which were analyzed in the final quadrupole to obtain MS^2 spectra. Panels **A**, **B**, and **C** represent MS^2 spectra obtained from first generation product ions at *m/z* 605, 579, and 577, respectively. These first generation product ions arise from loss of the sn-1, sn-3, or sn-2 substituents, respectively, as lithium salts from the parent $[M + Li]^+$ ion.

Figure 4B indicates that the most abundant product ion (*m/z* 303) from the $[M + Li - R_3CO_2H]^+$ ion is also generated by loss of the sn-2 substituent as an α,β-unsaturated fatty acid. In addition, $[R_2'CH{=}CHCO_2H + Li]^+$ (*m/z* 287), $[R_2CO_2H + Li]^+$ (*m/z* 289), and $[R_1CO_2H + Li]^+$ (*m/z* 263) ions are observed. Figure 4C indicates that the $[M + Li - R_2CO_2H]^+$ ion can undergo loss of either the sn-1 or the sn-3 substituent as an α,β-unsaturated fatty acid to yield ions of approximately equal abundance at *m/z* 331 and 303, respectively. The observations in Figure 4 indicate that ions reflecting combined losses of an outer (sn-1 or sn-3) fatty acid substituent and the sn-2 substituent can arise from initial loss of either an outer position substituent or the sn-2 substituent as a free fatty acid, followed by loss at the other adjacent position. The second substituent eliminated in this sequence is lost as an α,β-unsaturated fatty acid. Source CAD-MS^2 experiments with the lithiated adduct of the positional isomer (16:0/18:0/18:1)-TAG yielded similar findings (Figure 5).

The source CAD-MS^2 spectra in Figures 4 and 5 indicate that acylium ions of the fatty acid substituents observed in the tandem spectra of lithiated adducts in TAG do not arise from $[M + Li - R_nCO_2H]^+$ ions because acylium ions are not observed in these spectra. The source CAD-MS^2 spectra in Figure 6 indicate that the acylium ions rather arise from $[M + Li - R_2CO_2Li]^+$ ions. To obtain these spectra, the lithiated adduct of (16:0/18:0/18:1)-TAG was subjected to source CAD, and the fragment ions $[M + Li - R_1CO_2Li]^+$ (panel A), $[M + Li - R_3CO_2Li]^+$ (panel B), or $[M + Li - R_2CO_2Li]^+$ (panel C) were isolated in the first quadrupole and subjected to CAD in the collision cell to yield second generation fragment ions. In panels A and B, either the R_3CO^+ (*m/z* 265) or the R_1CO^+ (*m/z* 239) ion, respectively, but not both, are observed, and, in each case, that ion is substantially more abundant than the R_2CO^+ ion (*m/z* 267). In panel C, both R_1CO^+ (*m/z*

239) and R_3CO^+ (*m/z* 265) ions are observed in approximately equal abundance, and the R_2CO^+ ion (*m/z* 267) is absent, as expected. These findings indicate that acylium ions are preferentially generated from an outer fatty acid substituent and arise from a precursor ion generated by prior loss of another fatty acid substituent as its lithium salt.

Abundant fragment ions in the *m/z* range from 30 to 200 are also observed in the spectra in Figure 6. These include a series of alkyl ions at *m/z* 43, 57, 71, etc., and unsaturated series (e.g., 95, 109, etc. and 121, 135, etc.). Similar ion series observed under electron impact conditions are produced from alkyl chains by charge-driven fragmentation mechanisms [9]. The source CAD-MS^2 spectra in Figure 6 indicate that these ions arise from decomposition of $[M + Li - (R_nCO_2Li)]^+$ ions, and the source CAD-MS^2 spectra in Figures 4 and 5 indicate that such ions are not produced in high abundance from decomposition of $[M + Li - (R_nCO_2H)]^+$ ions. Although these ion series do not identify the locations of double bonds in unsaturated fatty acid substituents, the profile of ions in the *m/z* 30–200 range is virtually identical in Figure 6A, C but somewhat different in Figure 6B. The ions subjected to CAD in Figure 6A, C contain both saturated and unsaturated fatty acid substituents, whereas the ion subjected to CAD in Figure 6B contains only saturated fatty acid substituents.

Tandem Mass Spectra of Lithiated Adducts of TAG Species Containing Polyunsaturated Fatty Acid Substituents

The tandem spectra described above were obtained from lithiated adducts of TAG species containing only saturated or monounsaturated fatty acid substituents. We were unable to identify a source of standard TAG species that contain both a polyunsaturated fatty acid substituent and more than one distinct fatty acid species esterified to the same glycerol molecule. Commercially available trilinolein [(18:2/18:2/18:2)-TAG] and triarachidonin [(20:4/20:4/20:4)-TAG] were, however, analyzed by ESI/MS/MS as lithiated adducts under conditions of low-energy CAD, as illustrated in Figure 7.

The features of tandem spectra of lithiated adducts of (18:2/18:2/18:2)-TAG (Figure 7A) and of (20:4/20:4/20:4)-TAG (Figure 7B) were in general similar to those described above for TAG species that contained only saturated or monounsaturated fatty acid substituents. The spectra in both Figure 7A, B contain $[M + Li - (R_nCO_2H)]^+$ and $[M + Li - (R_nCO_2Li)]^+$ ions (at *m/z* 605 and 599 and at *m/z* 653 and 647, respectively), and both contain $[M + Li - (R_nCO_2Li) - (R'_{n\pm1}CH{=}CHCO_2H)]^+$ ions (at *m/z* 327 and at *m/z* 351, respectively). Both spectra also contain $[RCO_2H + Li]^+$ ions (at *m/z* 287 and *m/z* 311, respectively). In Figure 7A, there is a prominent RCO^+ ion (at *m/z* 263), and in Figure 7B there is an $[RCO - H_2O]^+$ ion (at *m/z* 269).

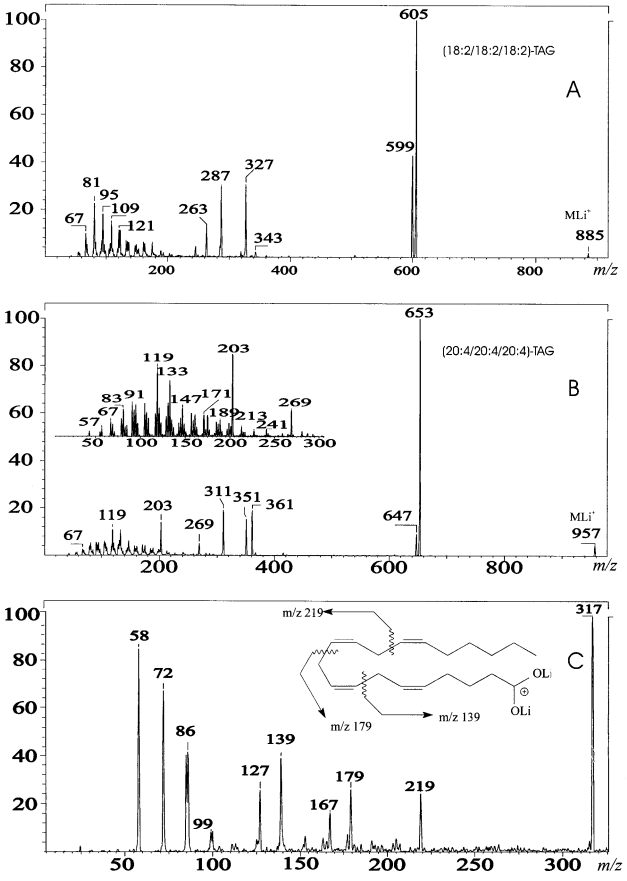

Figure 7. Tandem mass spectra of lithiated adducts of TAG species containing polyunsaturated fatty acid substituents and an MS^2 spectrum obtained after source CAD of triarachidonin that demonstrates double bond location in a polyunsaturated fatty acid substituent in the parent TAG molecule. Panel **A** is the tandem spectrum of the lithiated adduct of trilinolein [(18:2/18:2/18:2)-TAG] and panel **B** that of triarachidonin [(20:4/20:4/20:4)-TAG]. Panel **C** is an MS^2 spectrum obtained after subjecting (20:4/20:4/20:4)-TAG to source CAD, isolating the first generation fragment ion at *m/z* 317 in the first quadrupole, subjecting that ion to CAD in the collision cell, and analyzing second generation fragment ions in the final quadrupole.

One fairly prominent ion observed in Figure 7B that is not observed at comparable abundance in Figure 7A or spectra described earlier is that at *m/z* 361 representing loss of a substituted ketene from the $[M + Li - (R_nCO_2Li)]^+$ ion.

One difference between the tandem spectra of lithiated adducts of TAG species containing only saturated or monounsaturated fatty acid substituents compared to those of TAG species containing polyunsaturated fatty acid substituents is the ratio of ions reflecting loss of the free fatty acid or loss of its lithium salt from $[M + Li]^+$. This ratio is greater for polyunsaturated fatty acid substituents than for saturated or monounsaturated fatty acid substituents at a given collision energy. At a collision energy of 45 eV, the ratio of $[M + Li - (R_nCO_2H)]^+/[M + Li - (R_nCO_2Li)]^+$ is about 1.4 for saturated or monounsaturated fatty acids (Figure 1), about 2.3 for 18:2 (Figure 7A), and about 10 for 20:4

(Figure 7B). The collision energy also influences the $[M + Li - (R_nCO_2H)]^+/[M + Li - (R_nCO_2Li)]^+$ ratio. For saturated and monounsaturated fatty acid substituents, this ratio is about 1.4 at a collision energy of 45 eV and about 20 at a collision energy of 60 eV (not shown).

Determination of the Locations of Double Bonds in Polyunsaturated Fatty Acid Substituents of TAG by Source CAD-MS^2 Experiments

An interesting feature of source CAD experiments with lithiated adducts of TAG species is that $[R_nCO_2Li_2]^+$ ions are generated when TAG molecules are infused into the ion source in solutions containing 2 mM lithium acetate. Such ions are not observed when a low offset potential is applied to the skimmer but become readily apparent at skimmer potentials between 50 and 60 V. This indicates that the $[R_nCO_2Li_2]^+$ ions arise from fatty acid substituents esterified within TAG molecules and not from contaminating free fatty acids. The generation of $[R_nCO_2Li_2]^+$ ions from TAG species under source CAD conditions creates the opportunity to isolate these ions in the first quadrupole, subject them to CAD in the collision cell, and to analyze the product ions in the final quadrupole in order to examine the double bond location in unsaturated fatty acid substituents. Such an experiment is illustrated in Figure 7C for (20:4/20:4/20:4)-TAG. An ion at *m/z* 317 representing dilithiated 20:4 generated in the ion source was subjected to CAD, and the resultant MS^2 spectrum is displayed in Figure 7C. This spectrum identifies the fatty acid substituent as arachidonic acid by comparison to the tandem spectrum for standard arachidonic acid analyzed by ESI/MS/MS as its dilithiated adduct in the companion manuscript [46]. Similar source CAD-MS^2 experiments with (18:2/18:2/18:2)-TAG yielded a tandem spectrum of the dilithiated adduct of 18:2 that demonstrated that (9,12)-18:2 (linoleic acid) is the fatty acid substituent in this TAG species (not shown). Under source CAD conditions, $[RCO_2HLi]^+$ ions are also generated from triacylglycerol species, but tandem spectra of these monolithiated ions are not informative with respect to double bond location.

Discussion

Proposed Pathways for the Genesis of the Major Fragment Ions Observed in the Tandem Mass Spectra of Lithiated Adducts of Triacylglycerol Species

Scheme **1** proposes routes for sequential elimination of an outer (sn-1 or sn-3) fatty acid substituent and of the sn-2 substituent from lithiated adducts of TAG that are supported by studies with deuterium-labeled TAG species and with source CAD-MS^2 experiments described above. In the proposed routes, the first substituent is eliminated as a free fatty acid and the second as an α,β-unsaturated fatty acid. Scheme **1**A rationalizes a sequence in which an outer (sn-1 or sn-3) substituent is first eliminated as a free fatty acid and the sn-2 substituent is next eliminated as an α,β-unsaturated fatty acid. Scheme **1**B rationalizes an alternate sequence involving initial loss of the sn-2 substituent as a free fatty acid followed by loss of an outer substituent as an α,β-unsaturated fatty acid.

Studies described above with deuterium-labeled TAG indicate that the hydrogen atom on the carboxylic acid moiety in a substituent eliminated as free fatty acid derives from the α-methylene group of an adjacent fatty acid substituent rather than from a hydrogen atom bonded to a glycerol carbon atom. When the first fatty acid substituent is eliminated from an outer (sn-1 or sn-3) position, Scheme **1**A proposes that a five-membered cyclic intermediate structure then forms as a consequence of this hydrogen abstraction. The members of this cyclic intermediate include the sn-2 carbon of the glycerol backbone, the outer (sn-1 or sn-3) carbon of the glycerol backbone to which the expelled fatty acid had been esterified, carbon atom 1 in the fatty acid side chain of the sn-2 substituent, and both oxygen atoms bonded to that carbon atom. This intermediate structure then decomposes to eliminate the sn-2 substituent as a neutral α,β-unsaturated fatty acid, and the charge is retained by the remaining fragment, which is the lithiated adduct of the allyl ester of the remaining outer fatty acid substituent. Alternatively, the α,β-unsaturated fatty acid may be expelled as a lithium complex from the cyclic-five membered intermediate structure (Scheme **1**A).

As indicated in Scheme **1**B, a similar mechanism can be used to rationalize initial elimination of the sn-2 substituent as a free fatty acid, followed by elimination of either the sn-1 or the sn-3 substituent as an α,β-unsaturated fatty acid. As indicated in both Scheme **1**A, B, acylium ions are proposed to arise from other routes, which involve initial elimination of the lithium salt of a fatty acid substituent from $[M + Li]^+$. The acylium ion is then liberated from $[M + Li - (R_nCO_2Li)]^+$ ions by a mechanism which favors formation of acylium ions from the sn-1 or sn-3 substituents over the sn-2 substituent. These schemes propose plausible structures for intermediates in the genesis of major fragment ions observed in tandem mass spectra of lithiated adducts of TAG species and are consistent with features of tandem spectra of lithiated adducts of TAG species containing deuterium-labeled fatty acid substituents and with information provided about the sequence of fragment ion formation obtained from source CAD-MS^2 experiments. Among the features of these schemes that are consistent with the tandem mass spectra are that, when two fatty acid substituents are eliminated from the lithiated adduct of a TAG species, they are always adjacent substituents and therefore always include the sn-2 substituent. Fragment ions reflecting combined loss of the sn-1 and sn-3 substituent but not of the sn-2 substituent are not observed in any spectrum in which all combinations

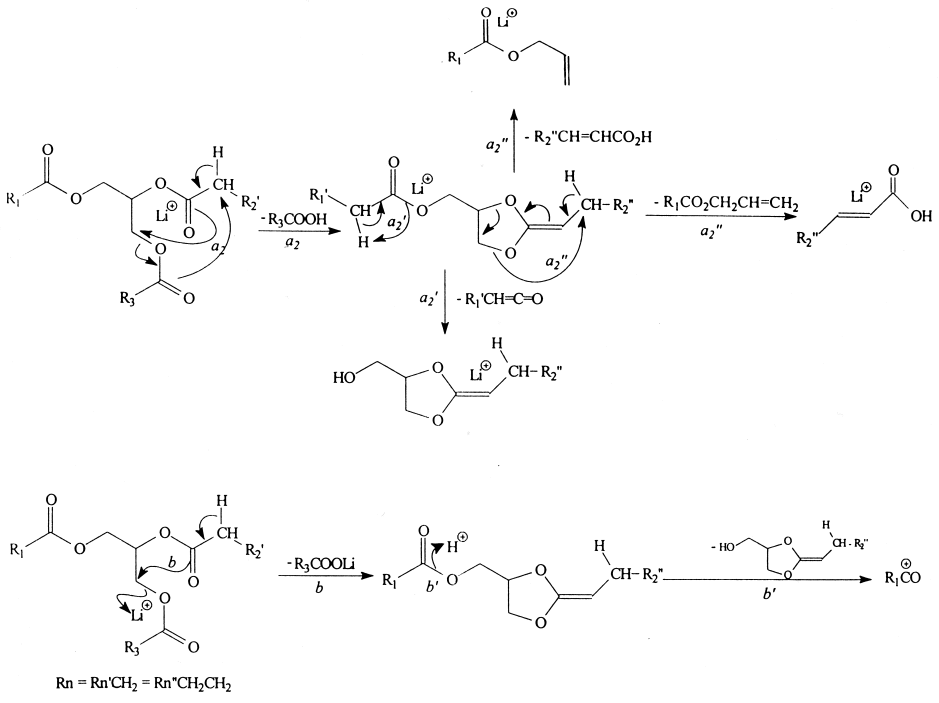

Scheme 1A

Scheme 1. Proposed pathways in the genesis of the major fragment ions observed in the tandem mass spectra of lithiated adducts of triacylglycerol species. **A** rationalizes formation of fragment ions arising from initial elimination of the sn-1 or sn-3 fatty acid substituent in triacylglycerol species as a free fatty acid (upper portion of scheme) or as a lithium salt (lower portion of scheme). **B** rationalizes formation of fragment ions arising from initial elimination of the sn-2 fatty acid substituent as a free fatty acid (upper portion of scheme) or as a lithium salt (lower portion of scheme). In **A**, the structure of the allyl ester of the sn-1 substituent is drawn that results from sequential elimination of the sn-3 fatty acid substituent as a free fatty acid (step a_2) and then of the sn-2 substituent (step a_2'') as an α,β-unsaturated fatty acid. Analogous allyl esters formed in **B** are designated $[MLi^+ - R_2CO_2H - R_n''CH{=}CHCO_2H]$, where $n = 1$ or $n = 3$, but the structures of these esters are not drawn in B.

of losses of two substituents can be distinguished by *m/z* values of product ions.

Identification of the sn-2 Substituent in Triacylglycerol Species from the Relative Abundances of Fragment Ions in the Tandem Mass Spectra of Lithiated Adducts

Several features of tandem mass spectra of lithiated adducts of TAG permit assignment of the sn-2 substituent. These include the facts that $[M + Li - (R_nCO_2H)]^+$ ions are of approximately equal abundance for $n = 1$ and $n = 3$ but are less abundant for $n = 2$. The same relationships are observed with $[M + Li - (R_nCO_2Li)]^+$ ions and with the R_nCO^+ acylium ions. Another, and perhaps the most robust feature of these spectra that identifies the sn-2 substituent, is the presence of a pair of ions that reflect combined loss of the sn-2 substituent and of an adjacent substituent, with the first substituent eliminated as a free fatty acid and the second as an α,β-unsaturated fatty acid.

One member of this pair of ions reflects combined loss of the sn-1 and sn-2 substituents from $[M + Li]^+$, and the other member reflects combined loss of the sn-2 and sn-3 substituents. This ion pair is separated in *m/z* value by the difference in masses between the sn-1 and sn-3 substituents in the TAG species. Because the members of this pair represent lithium adducts of the allyl esters of the two outer fatty acid substituents, the molecular weights of the fatty acids corresponding to the outer substituents can be computed by subtracting 47 from the *m/z* values of the members of the ion pair. The value 47 represents the difference in mass between a hydrogen atom and the sum of the masses of a ($-CH_2CH{=}CH_2$) moiety and a lithium ion. This means of distinguishing the outer fatty acid substituents from the sn-2 substituent is less likely to be confounded by effects of polyunsaturation than is comparison of the relative abundances of $[M + Li - (R_nCO_2H)]^+$, $[M + Li - (R_nCO_2Li)]^+$, or R_nCO^+ ions for various values of *n*.

Identification of the sn-2 substituent provides a key feature of TAG structure. Because the sn-2 carbon on the glycerol backbone is the only asymmetric center in a TAG molecule, determination of the sn-2 substituent specifies the positions of the fatty acid substituents as completely as is possible by mass spectrometric meth-

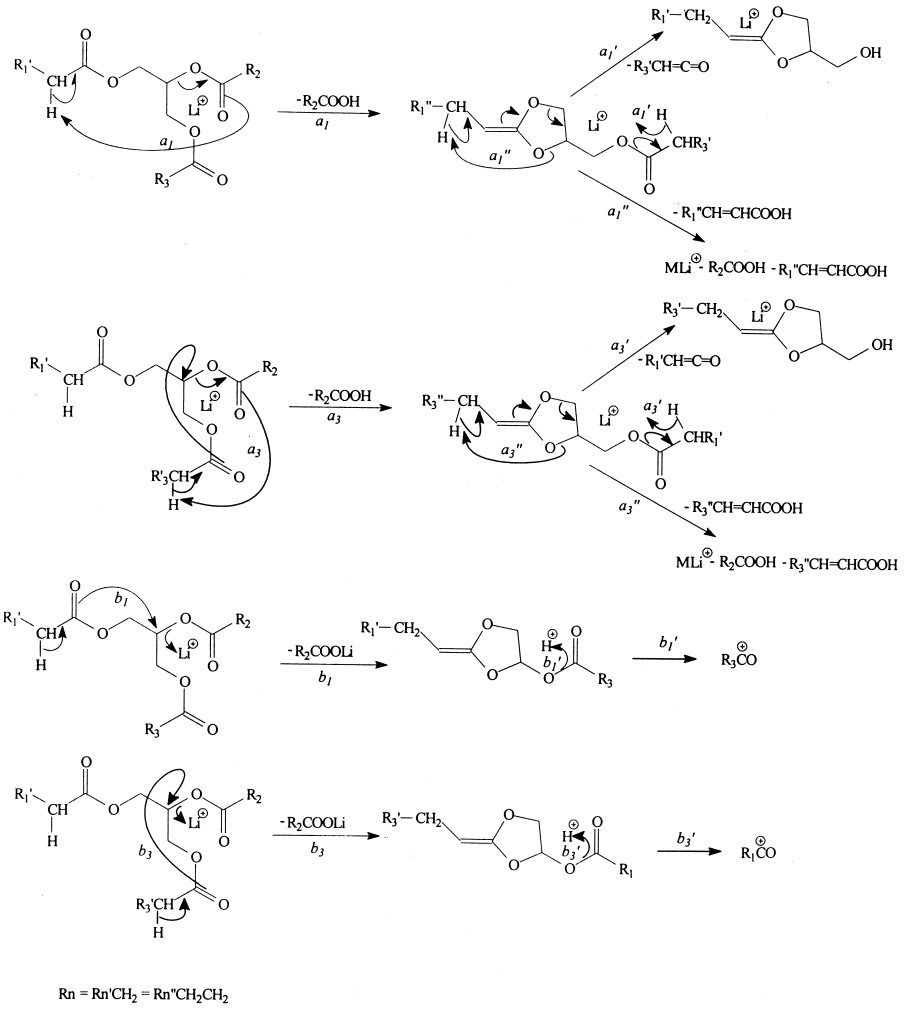

Scheme 1B

ods. TAG molecules that differ only with respect to the placement of the sn-1 and sn-3 substituents, such as (A/B/C)-TAG vs. (C/B/A)-TAG, where A, B, and C are distinct fatty acid residues, are enantiomers and cannot be distinguished by mass spectrometric methods alone. Such distinction would require the involvement of a second chiral center at some point in the analysis, such as using a chiral-phase separation technique before introduction of the analytes into the mass spectrometer.

Preferential Elimination of Polyunsaturated Fatty Acid Substituents as Free Fatty Acids from Lithiated Adducts of Triacylglycerols

Fragment ions reflecting elimination of saturated or monounsaturated fatty acid substituents from lithiated adducts of TAG species as free fatty acids or as lithium salts occur with comparable abundance in the tandem spectra. In contrast, polyunsaturated fatty acids, such as linoleic acid and arachidonic acid, are preferentially eliminated as free fatty acids rather than as lithium salts, and the magnitude of this preference appears to increase with the degree of unsaturation. Effects of fatty acid unsaturation are also observed in elimination of the phosphocholine head group from lithiated adducts of GPC lipids in ESI/MS/MS under low-energy CAD conditions [37]. Lithium adducts of GPC species containing only saturated or monounsaturated fatty acids preferentially eliminate phosphocholine as a lithium salt, but GPC species containing polyunsaturated fatty acids preferentially eliminate phosphocholine as a protonated species [37]. We do not yet understand the basis for these phenomena, but they may reflect some interaction of lithium ions with polyunsaturated moieties under low-energy CAD conditions.

Determination of Double Bond Location in Polyunsaturated Fatty Acid Substituents in TAG Species by Source CAD-MS^2 Experiments

Generation of $[RCO_2Li_2]^+$ ions from TAG species under source CAD conditions was unexpected, but it provides the opportunity to determine double bond location in unsaturated fatty acid substituents using approaches described in the companion manuscript [46]. The genesis of these $[RCO_2Li_2]^+$ ions has not been characterized beyond the demonstration that these ions are CAD products and do not arise from contaminating free fatty acids. This is reflected by the fact that such ions are not

observed if a low offset potential is applied to the skimmer and that their production requires offset potentials in the range of 50–60 V. Production of these ions under source CAD conditions may involve initial elimination of R_nCO_2H or R_nCO_2Li as a neutral species from the TAG − Li^+ adduct and subsequent complexation of Li^+ with the neutral. As described in this paper, elimination of both of these neutral species is observed in the tandem spectra of TAG − Li^+ adducts, and, as described in the companion manuscript [46], formation of $[R_nCO_2Li_2]^+$ ions is observed upon ESI/MS analyses of free fatty acids infused into the ion source in solutions containing lithium acetate.

Although the precise mechanism for production of $[RCO_2Li_2]^+$ ions from TAG under source CAD conditions has not been elucidated, the generation of these ions has permitted us to assign double bond location in arachidonic acid and linoleic acid esterified to TAG molecules using features of the spectra discussed in the companion manuscript [46]. The ESI/MS/MS methods described here thus offer the opportunity to determine the identity of each fatty acid substituent in a TAG molecule, to determine the positions of the carbon atoms in the glycerol backbone to which the fatty acid substituents are esterified, and to determine the location of double bonds within polyunsaturated fatty acid substituents.

Differences in Fragmentation Patterns Between Lithiated and Sodiated Adducts of TAG upon Low-Energy CAD

Although TAG − Li^+ adducts undergo informative fragmentation upon low-energy CAD, TAG − Na^+ adducts do so less readily and yield a more limited array of informative fragment ions [34]. Similarly, Li^+ adducts of GPC lipids yield much more informative tandem mass spectra upon low-energy CAD [45] than do Na^+ adducts [47]. The Na^+ ion is observed in low-energy CAD tandem spectra of TAG − Na^+ adducts [34], but the Li^+ ion is not observed in tandem spectra of TAG − Li^+ adducts even at high collision energies (not shown). Less internal energy must be required to release Na^+ from a complex with TAG than is required to release Li^+, and this is also the case for complexes of fatty alcohols with these ions [48]. Different affinities of Na^+ and Li^+ for various lipid species may account for different low-energy CAD fragmentation patterns of lipids complexed with these ions.

Applications of TAG Structural Characterization by ESI/MS/MS

We find that the small quantities of TAG species from islets isolated from Zucker Diabetic Fatty (ZDF) rats [1–3] are readily characterized using methods described here, and we are determining whether changes in islet TAG composition accompany evolution of the insulin secretory defect in these animals.

Acknowledgments

This work was supported by grants from the US Public Health Service (P41-RR-00954, R37-DK-34388, P60-DK-20579, P01-HL-57-278) and the Juvenile Diabetes Foundation (No. 996003). We thank Alan Bohrer for excellent technical assistance.

References

1. Shimabukuro, M.; Ohneda, M.; Lee, Y.; Unger, R. H. Role of nitric oxide in obesity-induced beta cell disease. *J. Clin. Invest.* **1997,** *100*, 290–295.
2. Shimabukuor, M.; Koyami, K.; Lee, Y.; Unger, R. H. Leptin or troglitazone-induced lipopenia protects islets from interleukin 1β cytotoxicity. *J. Clin. Invest.* **1997,** *100*, 1750–1754.
3. Koyama, K.; Chen, G.; Want, M.-Y.; Lee, Y.; Shimabukuor, M.; Newgard, C. B.; Unger, R. H. Beta cell function in normal rats made chronically hyperleptinemic by adenovirus-leptin gene therapy. *Diabetes* **1997,** *46*, 1276–1280.
4. Chilton, F. H.; Murphy, R. C. Stimulated production and natural occurrence of 1,2-diarachidonoylglycerophosphocholine in human neutrophils. *Biochem. Biophys. Res. Commun.* **1987,** *145*, 1126–1133.
5. Chen, Y.; Golay, A.; Swislocki, A. M.; Reaven, G. Resistance to insulin suppression of plasma free fatty acid concentrations and insulin stimulation of glucose uptake in non-insulin-dependent diabetes mellitus. *J. Clin. Endocrinol. Metab.* **1987,** *64*, 17–27.
6. Golay, A.; Swislocki, A. L. M.; Chen, Y.; Reaven, G. M. Relationships between plasma free fatty acid concentration, endogenous glucose production, and fasting hyperglycemia in normal and non-insulin-dependent diabetes mellitus. *Metabolism* **1987,** *36*, 392–402.
7. Ramanadham, S.; Hsu, F.-F.; Bohrer, A.; Nowatzke, W.; Ma, Z.; Turk, J. Electrospray ionization mass spectrometric analysis of phospholipids from rat and human pancreatic islets and subcellular membranes. Comparison to other tissues and implications for membrane fusion in insulin exocytosis. *Biochemistry* **1998,** *37*, 4533–4567.
8. Hsu, F.-F.; Bohrer, A.; Turk, J. Electrospray ionization tandem mass spectrometric analysis of sulfatide. Determination of fragmentation patterns and characterization of molecular species expressed in brain and in pancreatic islets. *Biochim. Biophys. Acta* **1998,** *1392*, 202–216.
9. Murphy, R. C. Mass Spectrometry of Lipids. In *Handbook of Lipid Research*; Snyder, F., Ed.; Plenum: New York, 1993; Vol. 7, pp 213–243.
10. Demirbuker, M.; Blomberg, L. G.; Olsson, N. U.; Bergqvist, M.; Herslof, B. G.; Jacobs, F. A. Characterization of triacylglycerols in the seeds of Aquilegia vulgaris by chromatographic and mass spectrometric methods. *Lipids* **1992,** *27*, 436–441.
11. Kallio, H.; Laasko, P.; Huopalathi, R.; Linko, R. R.; Oksman, P. Analysis of butter fat triacylglycerols by supercritical fluid chromatography/electron impact mass spectrometry. *Anal. Chem.* **1989,** *61*, 698–700.
12. Evershed, R. P. High resolution triacylglycerol mixture analysis using high temperature gas chromatography mass spectrometry with a polarizable stationary phase, negative ion chemical ionization, and mass resolved chromatography. *J. Am. Soc. Mass Spectrom.* **1996,** *7*, 350–361.
13. Manninen, P.; Laakso, P.; Kallio, H. Separation of gamma and alpha linolenic acid containing triacylglycerols to capillary supercritical fluid chromatography. *Lipids* **1995,** *30*, 665–671.
14. Manninen, P.; Laakso, P.; Kallio, H. Method for characterization of triacylglycerols and fat-soluble vitamins in edible oils and fats by supercritical fluid chromatography. *J. Am. Oil Chem. Soc.* **1995,** *72*, 1001–1008.

15. Kallio, H.; Rua, P. Distribution of the major fatty acids of human milk between sn-2 and sn-1,3 positions of triacylglycerols. *J. Am. Oil Chem. Soc.* **1994,** *71*, 985–992.
16. Cheung, M.; Young, A. B.; Harrison, A. G. O^- and OH^- chemical ionization of some fatty acid methyl esters and triacylglycerols. *J. Am. Soc. Mass Spectrom.* **1994,** *5*, 553–557.
17. Laakso, P.; Kallio, H. Triacylglycerols of winter butterfat containing configurational isomers of monoenoic fatty acyl residues. II. Saturated dimonoenoic triacylglycerols. *J. Am. Oil Chem. Soc.* **1993,** *70*, 1173–1176.
18. Laakso, P.; Kallio, H. Triacylglycerols of winter butterfat containing configurational isomers of monoenoic fatty acyl residues. I. Disaturated monoenoic triacylglycerols. *J. Am. Oil Chem. Soc.* **1993,** *70*, 1161–1171.
19. Kallio, H.; Currie, G. Analysis of low erucic acid turnip rapeseed oils (Brassica campestris) by negative ion chemical ionization tandem mass spectrometry. A method giving information on the fatty acid composition in positions sn-2 and sn-1/3 of triacylglycerols. *Lipids* **1993,** *28*, 207–215.
20. Currie, G.; Kallio, H. Triacylglycerols of human milk: rapid analysis by ammonia negative ion tandem mass spectrometry. *Lipids* **1993,** *28*, 217–222.
21. Taylor, D. C.; Gibblin, E. M.; Reed, D. W.; Hogge, L. R.; Olson, D. J.; Mackenzie, S. L. Stereospecific analysis and mass spectrometry of triacylglycerols from arabidopsis thaliana (L.) Heynh. Columbia seed. *J. Am. Oil Chem. Soc.* **1995,** *72*, 305–308.
22. Huang, A. S.; Delano, G. M.; Pidel, A.; Janes, L. E.; Softly, B. J. Templeman, G. J. Characterization of triacylglycerols in saturated lipid mixtures with applications to SALATRIM 23CA. *J. Agric. Food Chem.* **1994,** *42*, 453–460.
23. Huang, A. S.; Robinson, L. R.; Gursky, L. G.; Profita, R.; Sabidong, C. G. Identification and quantification of SALATRIM 23CA. *J. Agric. Food Chem.* **1994,** *42*, 468–473.
24. Lehmann, W. D.; Kessler, M. Characterization and quantification of human plasma lipids from crude lipid extracts by field desorption mass spectrometry. *Biol. Mass Spectrom.* **1983,** *10*, 220–226.
25. Evans, N.; Games. D. E.; Harwood, J. L.; Jackson, A. H. Field desorption mass spectrometry of triglycerides and phosphoglycerides. *Biochem. Soc. Trans.* **1974,** *2*, 1091–1092.
26. Laakso, P.; Kallio, H. Optimization of the mass spectrometric analysis of triacylglycerols using negative ion chemical ionization with ammonia. *Lipids* **1996,** *31*, 33–42.
27. Stroobant, V.; Rozenberg, R.; el Monier, B.; Deffense, E.; de Hoffmann, E. Fragmentation of conjugate bases of esters derived from multifunctional alcohols including triacylglycerols. *J. Am. Soc. Mass Spectrom.* **1995,** *6*, 498–506.
28. Anderson, M. A.; Collier, L.; Dillipane, R.; Ayorinde, F. O. Mass spectrometric characterization of venonia glamensis oil. *J. Am. Oil Chem. Soc.* **1993,** *70*, 905–908.
29. Lamberto, M.; Saitta, M. Principal component analysis in fast atom bombardment-mass spectrometry of triacylglycerols in edible oils. *J. Am. Oil Chem. Soc.* **1995,** *72*, 867–871.
30. Hori, M.; Sahashi, Y.; Koike, S.; Yamaoka, R.; Sago, M. Molecular species analysis of polyunsaturated fish triacylglycerols by high performance liquid chromatography/fast atom bombardment mass spectrometry. *Anal. Sci.* **1994,** *10*, 719–724.
31. Evans, C.; Traldi, P.; Bambigiotti-Alberti, M.; Gianelli, v.; Coran, S. A.; Vincieri, F. F. Positive and negative fast atom bombardment mass spectrometry and collision spectroscopy in the structural characterization of mono-, di-, and triglycerides. *Biol. Mass Spectrom.* **1991,** *20*, 351–356.
32. Sundin, P.; Larsson, P.; Wesen, C.; Odham, G. Chlorinated triacylglycerols in fish lipids. Chromatographic and mass spectrometric studies of model compounds. *Biol. Mass Spectrom.* **1992,** *21*, 633–641.
33. Kim, H. Y.; Salem, N., Jr. Application of thermospray high performance liquid chromatography/mass spectrometry for the determination of phospholipids and related compounds. *Anal. Chem.* **1987,** *59*, 722–726.
34. Duffin, K. L.; Henion, J. D.; Shieh, J. J. Electrospray and tandem mass spectrometric characterization of acylglycerol mixtures that are dissolved in nonpolar solvents. *Anal. Chem.* **1991,** *63*, 1781–1788.
35. Cheng, C.; Gross, M. L.; Pittenauer, E. Complete structural elucidation of triacylglycerols by tandem sector mass spectrometry. *Anal. Chem.* **1998,** *70*, 4417–4426.
36. Myher, J. J.; Kuksis, A.; Geher, K.; Park, P. W.; Diersen-Schede, D. A. Stereospecific analysis of triacylglycerols rich in long-chain polyunsaturated fatty acids. *Lipids* **1996,** *31*, 207–215.
37. Pittenauer, E.; Aichinger, T.; de Hueber, K.; Bailer, J. Characterization of seed oils for potential technical use by HPLC. *Proceedings of the 44th ASMS Conference on Mass Spectrometry and Allied Topics*; Portland, OR, 1996; p 928.
38. Neff, W. E.; Byrdwell, W. C. Soybean oil triacylglycerol analysis by reversed phase high performance liquid chromatography coupled with atmospheric pressure chemical ionization mass spectrometry. *J. Am. Oil Chem. Soc.* **1995,** *72*, 1185–1191.
39. Byrdwell, W. C.; Emken, E. A. Analysis of triglycerides using atmospheric pressure chemical ionization mass spectrometry. *Lipids* **1995,** *30*, 173–175.
40. Neff, W. E.; Byrdwell, W. C. Triacylglycerol analysis by high performance liquid chromatography-atmospheric pressure chemical ionization mass spectrometry: Crepis alpina and Venonia galamensis seed oils. *J. Liquid Chromatogr.* **1995,** *18*, 4165–4181.
41. Byrdwell, W. C.; Neff, W. E. Analysis of genetically modified canola varieties by atmospheric pressure chemical ionization mass spectrometric and flame ionization detection. *J. Liquid Chromatogr.* **1996,** *18*, 2203–2225.
42. McIntyre, D.; Fisher, S. The characterization of di- and triglycerides in oils and fats by API LC/MS. *Proceedings of the 44th ASMS Conference on Mass Spectrometry and Allied Topics*; Portland, OR, 1996; p 289.
43. Byrdwell, W. C.; Emken, E. A.; Neff, W. E.; Odlof, R. O. Quantitative analysis of triacylglycerols using atmospheric pressure chemical ionization mass spectrometry. *Lipids* **1996,** *31*, 919–935.
44. Mottram, H. R.; Evershed, R. P. Structure analysis of triacylglycerol positional isomers using atmospheric pressure chemical ionization mass spectrometry. *Tetrahedron Lett.* **1996,** *37*, 8593–8596.
45. Hsu, F.-F.; Bohrer, A.; Turk, J. Formation of lithiated adducts of glycerophosphocholine lipids facilitates their identification by electrospray ionization tandem mass spectrometry. *J. Am. Soc. Mass Spectrom.* **1998,** *9*, 516–526.
46. Hsu, F.-F.; Turk, J. Distinction among isomeric unsaturated fatty acids as lithiated adducts by electrospray ionization mass spectrometry using low energy collisionally activated dissociation on a triple stage quadrupole instrument. *J. Am. Soc. Mass Spectrom.*, submitted.
47. Han, X.; Gross, R. W. Structural determination of picomole amounts of phospholipids via electrospray ionization tandem mass spectrometry. *J. Am. Soc. Mass Spectrom.* **1995,** *6*, 1202–1210.
48. Adams, J.; Gross, M. L. Energy requirements for remote charge site ion decompositions and structural information from collisional activation of alkali metal cationized fatty alcohols. *J. Am. Chem. Soc.* **1986,** *108*, 6915–6922.